THE ASTROPHYSICAL JOURNAL, 473:L21–L24, 1996 December 10

ULTRAVIOLET IMAGING OF NGC 3310: A MERGER-DRIVEN GLOBAL STARBURST

DENISE A. SMITH,[1,2] SUSAN G. NEFF,[2] GREGORY D. BOTHUN,[3] MICHAEL N. FANELLI,[4] JOEL D. OFFENBERG,[4] WILLIAM H. WALLER,[4] RALPH C. BOHLIN,[5] ROBERT W. O'CONNELL,[6] MORTON S. ROBERTS,[7] ANDREW M. SMITH,[2] AND THEODORE P. STECHER[2]
Received 1996 July 5; accepted 1996 September 26

ABSTRACT

We present the first far-ultraviolet (FUV; $\lambda \sim 1500$ Å) image of the nearby peculiar SAB(r)bc galaxy NGC 3310. The small 15″ (945 pc) diameter circumnuclear starburst ring is the most luminous structure, producing 30% of the total observed FUV luminosity. Diffuse emission from the inner disk ($20'' < R < 40''$) contributes another ~20% of the observed FUV flux. A linear feature (the "arrow") appears to be a star-forming tidal feature. A diffuse arc observed at optical wavelengths (the "bow") is not visible in the FUV and is probably a tidally induced shell composed of older stars. Mean star formation rates range from 0.031 $M_\odot$ yr^{-1} kpc^{-2} in the arrow to 2.1 $M_\odot$ yr^{-1} kpc^{-2} at the brightest FUV source. The striking similarity between the $R^{1/4}$ law behavior of the FUV and B-band surface brightness profiles, combined with the very blue colors of NGC 3310, strongly argues that the present morphology is the result of a global starburst triggered by a merger with a dwarf companion.

Subject headings: galaxies: individual (NGC 3310) — galaxies: interactions — galaxies: starburst — ultraviolet: galaxies

1. INTRODUCTION

With a global $B - V$ color of +0.32, the nearby peculiar SAB(r)bc galaxy NGC 3310 (D = 13.1 Mpc, H_0 = 75 km s^{-1} Mpc^{-1}) is one of the bluest spiral galaxies in de Vaucouleurs et al. (1991). The far-infrared luminosity ($L_{IR} = 1.1 \times 10^{10}$ $L_\odot$) indicates that the starburst in this galaxy is comparable to that of the "prototypical" starburst galaxy M82. The peculiar optical morphology of NGC 3310 is illustrated in Figure 1 (Plate L3) (see also van der Kruit & de Bruyn 1976, hereafter KB76; Balick & Heckman 1981, hereafter BH81; Duric et al. 1986; Schweizer & Seitzer 1988). The semistellar nucleus may be powered by a LINER (Heckman & Balick 1980) or by photoionization by hot stars (Pastoriza et al. 1993, hereafter P93). Tightly wound spiral arms form a luminous, ≈15″ (945 pc) diameter, circumnuclear ringlike structure and contain numerous Hα sources and near-ultraviolet (NUV) emitting compact stellar clusters (e.g., BH81; P93; Meurer et al. 1996, hereafter M96). The "jumbo" H II region located 12″ (760 pc) southwest of the nucleus is ~10 times more luminous in Hα than the 30 Doradus "supergiant" H II region in the Large Magellanic Cloud (BH81), and also harbors multiple NUV-bright clusters (M96). A linear feature known as the "arrow" (Walker & Chincarini 1967) extends from 65″ to 150″ from the nucleus at P.A. 300° and has been interpreted variously as a jet (Bertola & Sharp 1984) or a tidal feature (BH81; Mulder, van Driel, & Braine 1995). A diffuse arc of emission (the "bow") 100″ from the nucleus is thought to be a tidally induced shell (Schweizer & Seitzer 1988). Together, the bow, the arrow, the 1.″5 (100 pc) displacement between the dynamical and the stellar centers of mass (van der Kruit 1976), and the low metallicities of the nuclear H II regions (BH81) indicate that NGC 3310 probably accreted a gas-rich dwarf galaxy a few times 10^7 to ~10^8 years ago, and perhaps experienced a nuclear outburst ~10^7 years ago (e.g., BH81; Bertola & Sharp 1984; Schweizer & Seitzer 1988; Mulder et al. 1995).

NGC 3310 thus provides a superb opportunity to investigate the starburst phenomenon in a tidally disturbed system. In this Letter, we present the first far-ultraviolet (FUV; $\lambda \sim 1500$ Å) image of NGC 3310. The morphology of the FUV emission and its implications concerning the star formation properties of NGC 3310 are discussed below. Future work will focus on the star formation history of NGC 3310, as derived from a detailed comparison of the existing ultraviolet data with recently obtained optical and near-infrared observations.

2. OBSERVATIONS AND DATA REDUCTION

The Ultraviolet Imaging Telescope (UIT) observed NGC 3310 through the FUV B1 filter (λ_{eff} = 1520 Å; $\Delta\lambda$ = 354 Å) for 1130 s on 1995 March 11 as part of the Astro-2 mission on board the Space Shuttle *Endeavour*. The telescope, detectors, filters, data reduction, and calibration are fully described in Stecher et al. (1992) and Waller et al. (1995). The resulting data have a 40′ field of view, an image scale of 1.″14 pixel^{-1}, and a 3.″4 FWHM point-spread function. FUV photometric measurements herein are expressed in magnitudes according to the monochromatic system $m_\lambda = -2.5 \log f_\lambda - 21.1$, where the flux f_λ is in units of ergs s^{-1} cm^{-2} Å^{-1}.

A comparison B-band image was provided by Thronson & Bailey (1996). This image was obtained at the Lowell Observatory 1.1 m telescope with the Texas Instrument CCD array, a set of filters on loan from J. A. Tyson, and standard data reduction techniques. The resulting data are characterized by a scale of 0.″7 pixel^{-1} and ~4″ seeing. The flux calibration is provided by Walker & Chincarini (1967).

Photometry is performed by summing the observed flux

[1] National Research Council Postdoctoral Fellow.
[2] Laboratory for Astronomy and Solar Physics, Code 681, NASA/Goddard Space Flight Center, Greenbelt, MD 20771.
[3] Department of Physics, University of Oregon, 120 Willamette Hall, Eugene, OR 97403.
[4] Hughes STX Corporation, Laboratory for Astronomy and Solar Physics, Code 681, NASA/Goddard Space Flight Center, Greenbelt, MD 20771.
[5] Space Telescope Science Institute, 3700 San Martin Drive, Baltimore, MD 21218.
[6] Astronomy Department, University of Virginia, Charlottesville, VA 22903.
[7] National Radio Astronomy Observatory, Edgemont Road, Charlottesville, VA 22903.

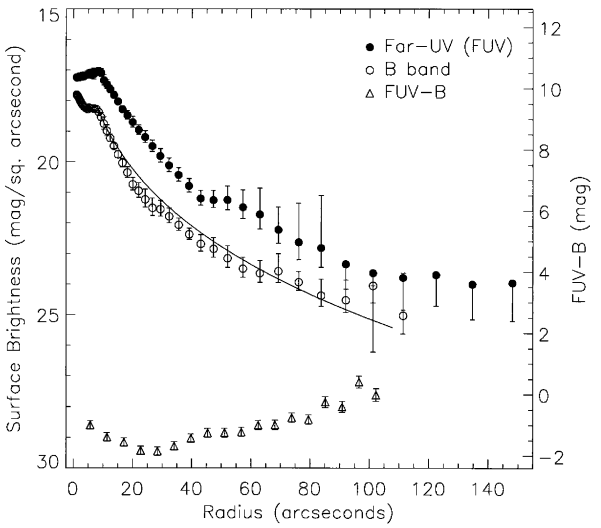

FIG. 3.—Surface brightness profiles, derived from the FUV and *B*-band emission as described in the main text. The radial FUV − *B* profile given by annular photometry is also displayed. The profiles have not been corrected for extinction. The solid line shows a $R^{1/4}$ law fit to the *B*-band emission between radii of 6″ and 96″, as derived from a 2.″32 pixel^{-1} scale *B*-band image. The fit to the inner portion of the galaxy is truncated at a radius of 8″, where the *B*-band emission flattens.

within a circular aperture centered upon the source of interest. Sky backgrounds are determined from measurements of several blank sky regions. Surface brightnesses profiles are computed with the STSDAS ELLIPSE task within IRAF[8] (e.g., Jedrzejewski 1987).

3. FAR-ULTRAVIOLET MORPHOLOGY

The FUV image of NGC 3310 is shown in Figure 2 (Plate L4). Radial profiles of the FUV and *B*-band surface brightnesses are presented in Figure 3. These figures reveal several important characteristics, as discussed below.

3.1. *The Nucleus* ($R \lesssim 5''$)

The nucleus of NGC 3310 is not a distinct source in the FUV, yet it is clearly visible in optical images with similar spatial resolution. A 1.″5 spatial resolution optical spectrum of the nucleus indicates the presence of hot ionizing stars (P93); these stars must emit at ultraviolet wavelengths. A 22″ field of view image obtained with the Faint Object Camera (FOC) and the F220W filter aboard the *Hubble Space Telescope*[9] (*HST*) (see M96), smoothed and rebinned to match the resolution of the UIT data, shows that the nucleus is in fact visible, although not prominent, at 2200 Å.

Together, measurements of the Hα/Hβ recombination line ratio (P93) and the extinction law of Kinney et al. (1994) imply a FUV optical depth of $A_{\rm FUV} = 4.1$ mag toward the nucleus, assuming a foreground dust screen (see M96 for a discussion of relevant reddening laws and geometries). At these optical depths, the nucleus would have to be at least ∼10 times more luminous than the jumbo H II region ($A_{\rm FUV} = 1.9$ mag) in order to be recognizable in the UIT image. Continuum and line fluxes measured by P93 indicate that this is not the case, however. With the caveat that Balmer decrements may overestimate the continuum extinction (Calzetti, Kinney, & Storchi-Bergmann 1994), we conclude that the apparent lack of FUV emission is primarily due to extinction. Multiwavelength continuum observations will be used to reexamine this issue in a follow-up study.

[8] IRAF is distributed by the National Optical Astronomy Observatories, which are operated by AURA, Inc., under a cooperative agreement with the National Science Foundation.

[9] Based on observations with the NASA/ESO *Hubble Space Telescope*, obtained at the Space Telescope Science Institute, which is operated by the Association of Universities for Research in Astronomy, Inc., under NASA contract NAS 5-26555.

3.2. *The Starburst "Ring"* ($5'' \lesssim R \lesssim 10''$)

Figure 2 indicates that the starburst "ring" is the strongest organized source of FUV emission in NGC 3310; 30% of the total observed FUV emission is produced within a radius of 10″. At redshifts of $z \sim 2$–3, this structure would be confined to a region ≈0.″2 in diameter for $\Omega = 1$ and would appear pointlike in low-resolution observations. In the absence of diagnostic spectroscopy, a high-redshift NGC 3310–like object consequently could be mistaken for an active galactic nucleus (AGN).

Since ultraviolet and Hα wavelengths are direct and indirect tracers of massive stars, respectively, a comparison of their morphologies can provide important clues regarding the properties of the associated star-forming regions. In the case of NGC 3310, the FUV and Hα (BH81; P93) morphologies of the ringlike structure are similar, but not identical. In particular, the jumbo H II region is not the brightest FUV source. The brightest region of FUV emission, "FUV1," is instead located to the east of the Hα source identified as H II region "B" by P93. The H II region B itself does not appear to be a distinct source at FUV wavelengths. Since Hα and FUV wavelengths have different sensitivities to extinction and to the relative mix of O and B stars, the relative variations in the FUV and Hα surface brightnesses are most likely due to changes in the optical depth and/or the stellar populations. The relative weakness of the Hα emission in the FUV-bright region may indicate that the ionizing stars have evolved off the main sequence. Alternatively, the brightest FUV source may simply represent a local minimum in the optical depth. A comparison between the FUV and NUV morphologies of the southern portion of the ring, as depicted by the UIT and the smoothed *HST* FOC images, suggests that region B is redder than region FUV1. This additional evidence implies that the brightest FUV emission source corresponds to a hole in the dust distribution, since the FUV − NUV color is relatively constant as a function of age (Hill et al. 1995). Multiwavelength imagery and/or spectroscopy obtained with similarly high spatial resolutions is needed to further constrain the relative optical depths, ages, and locations of these star-forming regions.

3.3. *The Inner Disk* ($10'' \lesssim R \lesssim 40''$)

The FUV and Hα emission from "normal" spiral galaxies is generally confined to star-forming regions located in the spiral arms, as in the "beads on a string" effect (e.g., Hill et al. 1992; Chen et al. 1992). The Hα emission from NGC 3310 is generally consistent with this picture (e.g., BH81). At FUV wavelengths, however, the inner disk of NGC 3310 exhibits diffuse emission. NGC 3310 is not unique: the starburst/Seyfert 2 galaxy NGC 1068 is also characterized by a FUV-bright disk (Neff et al. 1994). Further FUV observations are needed to determine the frequency with which FUV-bright disks are found in starburst systems; such studies would aid the

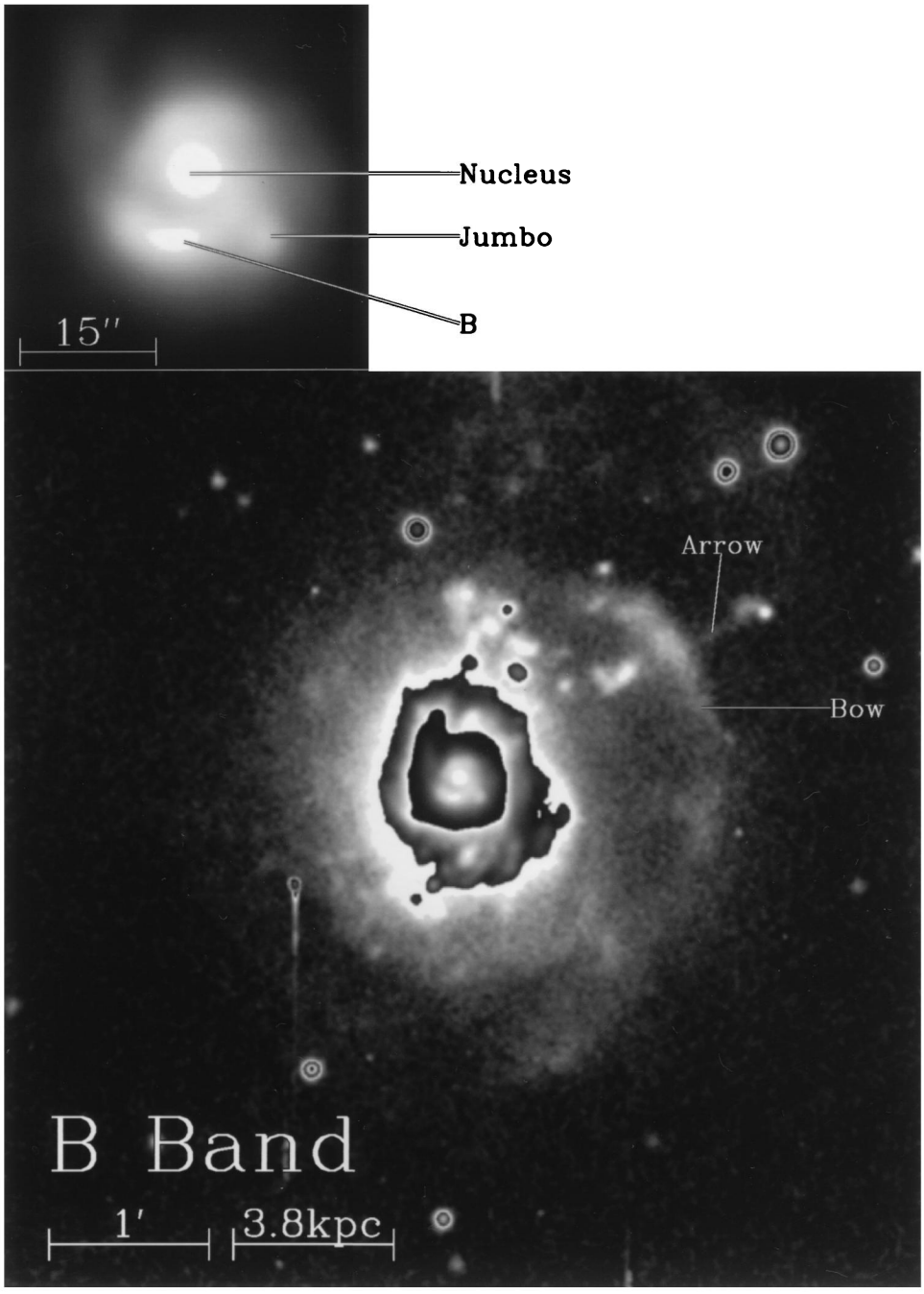

FIG. 1.—NGC 3310: optical. This *B*-band image illustrates the optical morphology of NGC 3310. The image has been wrapped three times; east is to the left, and north is up. Some field stars are saturated. The central ≈40″ is shown at an expanded scale in the upper left. A diffuse arc of emission (the "bow") and a linear feature (the "arrow") are observed in the peripheral regions of the galaxy.

SMITH et al. (see 473, L21)

PLATE L4

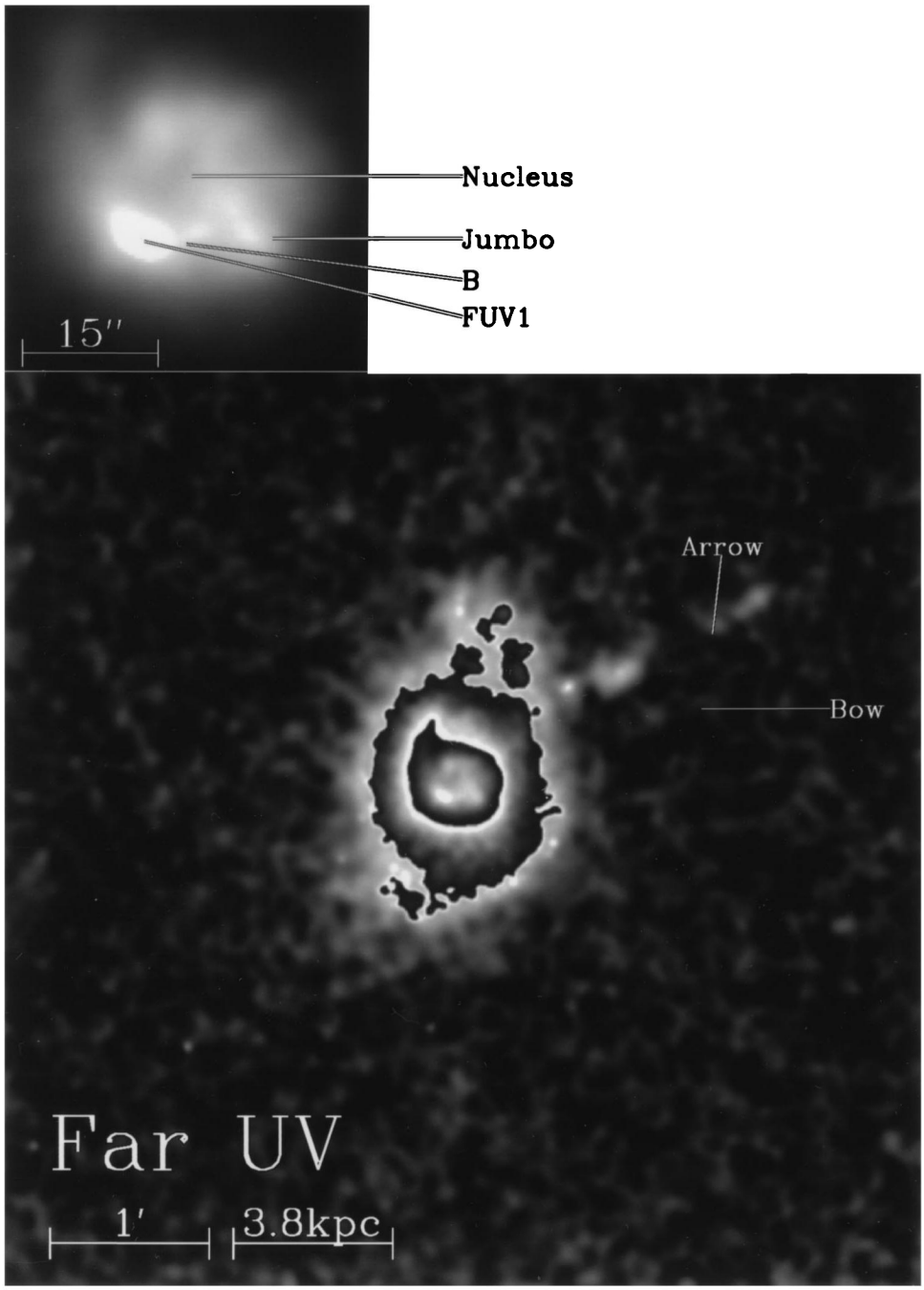

FIG. 2.—NGC 3310: far-ultraviolet (FUV). This image, obtained by the Ultraviolet Imaging Telescope, is the first ~arcsecond resolution FUV image of NGC 3310. The image is displayed as in Fig. 1. The circumnuclear starburst ring dominates the FUV morphology. The disk of NGC 3310 and the arrow are also sources of FUV emission. The semistellar nucleus and the bow are not detected in the FUV.

SMITH et al. (see 473, L22)

TABLE 1

STELLAR CONTENT

Source (1)	Θ (2)	M_{FUV} (3)	FUV − B (4)	N (5)	Mass (6)	SFR (7)	SFRA (8)
Southern arm	11.3	−20.85	−1.26 ± 0.13	1990	22.6	0.83	2.09
Jumbo	11.3	−20.59	−1.33 ± 0.14	1570	17.8	0.65	1.64
Northern knots	11.3	−17.06	−1.79 ± 0.22	61	0.69	0.025	0.064
Arrow	11.3	−16.27	−1.36 ± 0.26	29	0.33	0.012	0.031
Bow	11.3	−14.32	−0.46 ± 0.47	0.69	0.055	0.0020	0.0051
Global	204	−23.40	−1.40 ± 0.13	20,860	236	8.6	0.066

NOTE.—Columns (3), (5), (6), (7), and (8) are corrected for $A_{FUV} = 2.41$ mag of extinction.

Col. (1).—Aperture locations (J2000) are as follows: southern arm: R.A. = $10^h38^m46\overset{s}{.}0$ decl. = +53°30′4″.4, includes FUV1 and B; jumbo: R.A. = $10^h38^m44\overset{s}{.}9$ decl. = +53°30′5″.7; northern knots: quantities reflect the average flux measured for knots located between P.A. ~330° and ~350°; arrow: R.A. = $10^h38^m38\overset{s}{.}4$ decl. = +53°30′55″.4, refers to the inner portion of the arrow; bow: R.A. = $10^h38^m36\overset{s}{.}6$ decl. = +53°31′8″.2, measurements are upper limits; global: R.A. = $10^h38^m45\overset{s}{.}82$ decl. = +53°30′12″.5.

Col. (2).—Diameter of circular aperture used for all measurements, in arcseconds. 11″.3 = 710 pc; 204″ = 3′.4 = 12.9 kpc.

Col. (3).—Absolute FUV magnitude.

Col. (4).—FUV − B color in magnitudes.

Col. (5).—Equivalent number of 30 Doradus regions, assuming 30 Doradus is characterized by $M_{FUV} = -12.6$ without extinction corrections and $D_{LMC} = 52.5$ kpc (Israel & Koornneef 1979).

Col. (6).—Equivalent stellar mass in units of $10^7\ M_\odot$, assuming a constant star formation rate.

Col. (7).—Mean star formation rate, in units of $M_\odot\ yr^{-1}$.

Col. (8).—Mean star formation rate per unit area, in units of $M_\odot\ yr^{-1}\ kpc^{-2}$.

interpretation of high-redshift systems, which have observed optical emissions corresponding to the rest-frame FUV.

Furthermore, "normal" disk galaxies such as M74 and M33 exhibit exponential surface brightness profiles with scale lengths that are longer in the FUV than in the optical (Cornett et al. 1994). The fact that NGC 3310's FUV and B-band surface brightness profiles (Fig. 3) are not characterized by exponential behavior suggests that the structure of NGC 3310 is anomalous. Independent surface photometry by one of us (G. B.) on a B-band frame of NGC 3310 at 2″.32 pixel^{-1} confirms the general nature of the surface brightness profile shown in Figure 3 and shows that this profile is well fitted by a $R^{1/4}$ law. The remarkable similarity between the FUV and B-band profiles strongly suggests that a global starburst has occurred, and has resulted in the $R^{1/4}$ profile that is a manifestation of mergers and dissipation. Unless the dust properties are significantly different from those observed in the Milky Way, it is very unlikely that the similar luminosity profiles are the result of scattering effects associated with a starburst in the inner regions (e.g., $R < 40''$), since forward scattering dominates at FUV wavelengths (Witt et al. 1992). We therefore conclude that the structural similarity between the B and FUV profiles, combined with the very blue color throughout NGC 3310, argues that the present morphology is a result of a merger with a dwarf companion that has triggered a global starburst. FUV imagery indicates that NGC 4214 may represent an analogous situation (Fanelli et al. 1996).

3.4. *The Outer Regions* ($R \gtrsim 40''$)

Many, but not all, of the optical features associated with the outer regions of NGC 3310 are also sources of FUV emission: five knots between P.A. ~330° and P.A. ~350° and the arrow are visible in the FUV. In contrast, the bow is not detected in the FUV.

The five northern knots appear to be sites of recent star formation. An archival *HST* image taken with the WFPC2 and F606W filter (see footnote 9) resolves these knots into stellar clusters with FWHM of ~40 pc. Together, the presence of FUV and Hα emission (KB76) associated with stellar clusters implies that the knots are recent sites of massive star formation and regions of low optical depth. The similarity between the average FUV − B color of the knots and that of the inner disk indicates that these regions of star formation activity may be characterized by similar ages and optical depths. These knots do not form organized structures, and their spatial distribution may reflect star formation triggered by tidal disturbances in the outer portions of the galaxy (KB76).

The arrow appears to be a star-forming tidal feature. First, the H I properties of the arrow are best explained in terms of a tidal feature (Mulder et al. 1995). Stellar clusters are visible in the portion of the arrow covered by the WFPC2 field of view; a possible detection of Hα emission is reported by KB76. The stellar clusters most likely contain young massive stars which are responsible for the observed FUV and Hα emission. The FUV − B colors of the arrow and the starburst ring imply that these areas may have similar ages and optical depths. The observed star formation may have been triggered by tidal processes, or the gas may simply have a surface density naturally exceeding that necessary for star formation.

Finally, the fact that the bow observed in optical continuum images is *not* FUV-bright suggests that it contains older late-type stars. The fact that the age of this feature, rather than its brightness, is responsible for the lack of FUV emission is confirmed by measurements of the bow at the location where it crosses the arrow in the optical (see Table 1). These data indicate that the bow is significantly redder than the other regions exhibiting FUV emission. Our hypothesis is also consistent with the apparent lack of Hα emission from this region (KB76). Together, the morphology of the bow and the apparent lack of recent star formation suggest that this feature consists of material displaced from the outer regions of the original galaxy as a result of merger activity.

4. STELLAR CONTENT

The star formation properties of NGC 3310 are constrained via an evolutionary spectral synthesis code (Landsman 1996).

Model spectra are generated for a constant star formation rate using the Schaller et al. (1992) and Schaerer et al. (1993) evolutionary tracks coupled with the Kurucz (1992) atmospheric models and appropriate filter response functions. An instantaneous burst is also considered. Our calculations assume a stellar initial mass function (IMF) with a power-law slope of -1.35 (a Salpeter IMF) and a metallicity of $Z = 0.4$ $Z_\odot$ (P93). The lower and upper mass cutoffs of the IMF are taken to be $m_l = 0.1$ $M_\odot$ and $m_u = 110$ $M_\odot$, respectively. The global FUV $-$ U, $U - B$, and $B - V$ colors of NGC 3310 (de Vaucouleurs et al. 1991), the reddening laws of Kinney et al. (1994) and Savage & Mathis (1979), and a foreground screen (see also § 3.1) are used with the models to determine the average age and the average optical depth of the burst. Table 1 and Figure 3 indicate that spatial variations in the FUV $- B$ colors of NGC 3310 are relatively small, so that application of a global extinction correction is reasonable. We find average burst ages and optical depths of 270 Myr and $A_V = 0.67$ mag for a constant star formation rate, and 15 Myr and $A_V = 0.63$ mag for an instantaneous burst. These ages are consistent with the age of the proposed merger event (see § 1). Since a 15 Myr old instantaneous burst will not contain enough O stars to produce the observed Hα emission, we adopt the case of constant star formation in the discussion below.

Based upon the absolute extinction-corrected FUV magnitudes given in Table 1, we find time-averaged star formation rates ranging from 0.031 $M_\odot$ yr^{-1} kpc^{-2} in the arrow to 2.1 $M_\odot$ yr^{-1} kpc^{-2} in the vicinity of sources FUV1 and B. The global star formation rate is 8.6 $M_\odot$ yr^{-1}. This current star formation activity heats the far-infrared emitting dust, as evidenced by the high dust temperature implied by NGC 3310's 60/100 μm flux ratio. The star formation rate associated with the global obscured FUV emission (7.7 $M_\odot$ yr^{-1}) is in fact in excellent agreement with that implied by the far-infrared emission ($dM/dt = 6.5 \times 10^{-10}$ $L_{\rm IR} \sim 7$ $M_\odot$ yr^{-1}; Thronson & Telesco 1986).

Finally, we note that M96 have used NUV data to estimate the stellar content within the central $\approx$25″ of NGC 3310. This region contains 35% of the total FUV flux, which corresponds to a stellar mass of 22×10^7 $M_\odot$ for constant star formation, and 84×10^7 $M_\odot$ for an instantaneous burst. Based upon star formation history conversion factors quoted by M96, we conclude that the FUV and NUV data are in agreement to within factors of 1.2–1.8. Given the inherent uncertainties in comparing data from such different instruments as the UIT and the *HST* and in modeling starburst stellar populations, we consider our data and models to be in good agreement with those of M96.

We thank the many people that contributed to the success of the Astro-2 mission, as well as an anonymous referee who provided several insightful comments that strengthened this paper. This work was performed while D. A. S. held a National Research Council–GSFC Research Associateship. R. W. O. acknowledges NASA support through grants NAG5-700 and NAGW-4106 to the University of Virginia. Funding for the UIT project has been through the Spacelab Office at NASA Headquarters under Project 440-51. We also wish to thank Harley Thronson and Brenae Bailey for providing their B-band image of NGC 3310. This research has made use of the NASA/IPAC Extragalactic Database (NED), which is operated by the Jet Propulsion Laboratory, Caltech, under contract with the National Aeronautics and Space Administration.

REFERENCES

Balick, B., & Heckman, T. M. 1981, A&A, 96, 271 (BH81)
Bertola, F., & Sharp, N. A. 1984, MNRAS, 207, 47
Calzetti, D., Kinney, A. L., & Storchi-Bergmann, T. 1994, ApJ, 429, 582
Chen, P. C., et al. 1992, ApJ, 395, L41
Cornett, R. H., et al. 1994, ApJ, 426, 553
de Vaucouleurs, G., de Vaucouleurs, A., Corwin, H. G., Buta, R. J., Paturel, G., & Fouqué, P. 1991, Third Reference Catalogue of Bright Galaxies (New York: Springer)
Duric, N., Seaquist, E. R., Crane, P. C., & Davis, L. E. 1986, ApJ, 304, 82
Fanelli, M. N., et al. 1996, ApJ, submitted
Heckman, T. M., & Balick, B. 1980, A&A, 83, 100
Hill, J. K., et al. 1992, ApJ, 395, L37
———. 1995, ApJ, 438, 181
Israel, F. P., & Koornneef, J. 1979, ApJ, 390, 403
Jedrzejewski, R. 1987, MNRAS, 226, 747
Kinney, A. L., Calzetti, D., Bica, E., & Storchi-Bergmann, T. 1994, ApJ, 429, 172
Kurucz, R. L. 1992, The Stellar Populations in Galaxies, ed. B. Barbuy & A. Renzini (Dordrecht: Kluwer), 225
Landsman, W. B. 1996, private communication
Meurer, G. R., Heckman, T. M., Leitherer, C., Kinney, A., Robert, C., & Garnett, D. R. 1995, AJ, 110, 2665 (M96)
Mulder, P. S., van Driel, W., & Braine, J. 1995, A&A, 300, 687
Neff, S. G., Fanelli, M. N., Roberts, L. J., O'Connell, R. W., Bohlin, R., Roberts, M. S., Smith, A. M., & Stecher, T. P. 1994, ApJ, 430, 545
Pastoriza, M. G., Dottori, H. A., Terlevich, E., Terlevich, R., & Diaz, A. I. 1993, MNRAS, 260, 177 (P93)
Savage, B. D., & Mathis, J. S. 1979, ARA&A, 17, 73
Schaerer, D., Meynet, G., Maeder, A., & Schaller, G. 1993, A&AS, 98, 523
Schaller, G., Schaerer, D., Meynet, G., & Maeder, A. 1992, A&AS, 96, 269
Schweizer, F., & Seitzer, P. 1988, ApJ, 328, 88
Stecher, T. P., et al. 1992, ApJ, 395, L1
Thronson, H., & Bailey, B. 1996, private communication
Thronson, H. A., & Telesco, C. M. 1986, ApJ, 311, 98
van der Kruit, P. C. 1976, A&A, 49, 161
van der Kruit, P. C., & de Bruyn, A. G. 1976, A&A, 48, 373 (KB76)
Walker, M. F., & Chincarini, G. 1967, ApJ, 147, 416
Waller, W. H., et al. 1995, AJ, 110, 1255
Witt, A. N., Petersohn, J. K., Bohlin, R. C., O'Connell, R. W., Roberts, M. S., Smith, A. M., & Stecher, T. P. 1992, ApJ, 395, L5